Weierstraß-Institut
für Angewandte Analysis und Stochastik

im Forschungsverbund Berlin e.V.

Preprint ISSN 0946 – 8633

Non-Raman redshift by pulse splitting in the normal dispersion regime

Ayhan Demircan[1],Marcel Kroh[2] ,Uwe Bandelow[1]

submitted: 19 March 2007

[1] Weierstrass Institute
for Applied Analysis and Stochastics
Mohrenstraße 39
10117 Berlin, Germany
E-Mail: demircan@wias-berlin.de
bandelow@wias-berlin.de

[2] Fraunhofer-Institute for Telecommunications
Heinrich-Hertz-Institute
Einsteinufer 37
10587 Berlin,Germany
E-Mail:kroh@hhi.de

No. 1218
Berlin 2007

2000 *Mathematics Subject Classification.* 35Q55,35Q60,78A60.

Key words and phrases. Nonlinear Schrödinger Equation, Optical Fiber.

This work was supported by DFG Research Center MATHEON.

Edited by
Weierstraß-Institut für Angewandte Analysis und Stochastik (WIAS)
Mohrenstraße 39
10117 Berlin
Germany

Fax: + 49 30 2044975
E-Mail: preprint@wias-berlin.de
World Wide Web: http://www.wias-berlin.de/

Abstract

While usually the generation of a Stokes component is attributed to Raman scattering, we present here experimentally and numerically a more fundamental mechanism which can be explained by the nonlinear Schrödinger equation alone. It can be employed to excite new frequency components on the red side, by using pulse splitting in the normal dispersion regime.

The nonlinear propagation of a pulse through an optical medium can result in considerable changes to its temporal and spectral properties, due to interplay of different physical effects acting on the pulse. For example the supercontinuum generation in nonlinear fibers has been a subject of numerous investigations for years, see e.g. the review [1], both because of the many applications of supercontinuum sources, as well as the interesting nonlinear physics that is involved in the spectral broadening process. There is a variety of effects leading to specific pulse and spectrum characteristics, like soliton fission (SF), associated with the generation of dispersive waves [2], modulation instability (MI) [3], Raman scattering, and other four-wave-mixing processes. This situation makes it particularly difficult to identify the impact of each physical process in a specific physical experiment. But SF and MI, which are described solely by the fundamental nonlinear Schrödinger equation (NLSE) in the anomalous dispersion regime with some perturbation, turn out to be the basic mechanisms. This reflects how inherent properties of the NLSE are of prime importance for the propagation dynamics, even for ultrashort pulse propagation in photonic-crystal fiber (PCF) with extremely high nonlinearity. To avoid the influence of MI and soliton effects, such as SF and self-frequency shift, the pump pulse can be injected within the normal dispersion regime far from the zero-dispersion wavelength. This enables one to investigate the effects of Raman-scattering. Additionally, the normal dispersion regime provides parameter regions where the efficiency of four-wave mixing is reduced and the signature of a discrete Raman cascade can be clearly identified. Also the role of cross-phase modulation (XPM) and parametric four-wave-mixing can be investigated [4, 5]. But the fundamental properties in the normal dispersion regime are suppressed or superimposed, so that it becomes difficult to isolate the relative contributions of the involved physical parameters. In this letter, we show for the first time that only dispersive effects are necessary to generate a spectral broadening to the red side. Already a small amount of third-order dispersion(TOD) in the normal dispersion regime can lead to a pulse-breakup above a certain pulse power. The splitting is followed by an expansion of the spectrum towards longer wavelengths and the evolution of a broad Stokes component without any impact of Raman scattering. The Stokes frequency depends strongly

on the third-order dispersion coefficient, enabling the transfer of energy to a broad range of longer wavelengths. To understand the underlying mechanisms leading to the red-shift, we have solved numerically the one-dimensional nonlinear Schrödinger equation Eq. (1) with only additionally TOD and fourth-order dispersion (FOD). We exclude in our numerical investigations any contribution from phase-matched parametric four-wave mixing and from higher-order nonlinearities as Raman scattering or self-steepening. This corresponds to the situation of a highly nonlinear fiber (HNLF), with pulse durations exceeding several picoseconds and small input powers so that the spectral bandwidth is much smaller than the Raman frequency shift in fused silica and the pump pulses do not suffer significantly from intrapulse Raman scattering as in the femtosecond case. It is assumed that the pulse propagates along the z-axis within a retarded time frame $\tau = t - z/v_g$, moving with the group velocity v_g of the pulse. The general form of the NLSE for the slowly varying complex envelope $A(z,\tau)$ of a pulse is given by

$$\frac{\partial A}{\partial z} = -\frac{i}{2}\beta_2\frac{\partial^2 A}{\partial \tau^2} + \frac{1}{6}\beta_3\frac{\partial^3 A}{\partial \tau^3} + \frac{i}{24}\beta_4\frac{\partial^4 A}{\partial \tau^4} + i\gamma|A|^2 A\,. \qquad (1)$$

Our technique for solution of Eq. (1) is based on a standard de-aliased pseudospectral method in which the dispersion parts are calculated in the frequency domain and the nonlinearity is calculated as a product in the time domain. The integration is performed for the whole equation in the frequency domain with an eigth-order Runge-Kutta integration scheme with adaptive stepsize control [6]. The experimen-

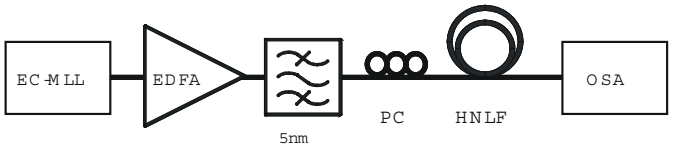

Figure 1: Experimental setup (abbreviations are defined in the text).

tal setup is shown in Fig. (1). A tunable mode-locked laser (EC MLL) was used to generate pulse trains with a repetition rate of 10 GHz with timing jitter smaller than 100 fs (between 100 Hz – 10 MHz), and 1535–1565 nm tuning range. The direct output of the EC MLL was amplified in a high-power erbium-doped fiber amplifier (EDFA), which has a maximum average output power of 26 dBm. A pulse with a $sech^2$ form is then propagated through a highly nonlinear fiber with a dispersion flattened profile to minimize the TOD. The dispersion and its slope at 1550 nm is approximately $D = -0.09\,ps/nm/km$ and $S = 0.019\,ps/nm^2/km$, respectively. The HNLF has its zero dispersion wavelength (ZDW) centered at $\lambda = 1555$ nm. The fiber is 789 m long and has a nonlinear coefficient of $\gamma = 10.5\,W^{-1}km^{-1}$, with a fiber loss of $0.84\,dB/km$. In particular, we will first consider propagation of an initially hyperbolic secant pulse $A(0,t) = \sqrt{P_0}sech(t/\tau_0)$ with $\tau_0 = 1.8ps$ injected at $\lambda_p = 1535nm$, along a fiber with dispersion coefficients $\beta_2 = 0.53ps^2/km$, $\beta_3 = 0.03ps^3/km$, $\beta_4 = 0$ and with nonlinear coefficient $\gamma = 10.5km^{-1}W^{-1}$ for conditions similar to those of

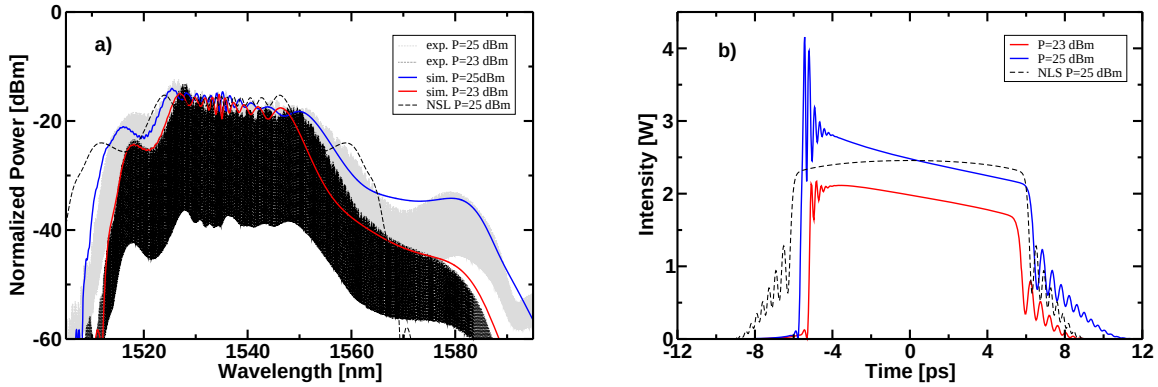

Figure 2: Spectra a) and pulse shapes b) for injected pulses with $sech^2$ forms with widths $\tau_0 = 1.8ps$ and average powers P_{IN} of $23.0dBm$ and $25dBm$ after the HNLF at $\lambda_p = 1535nm$ with dispersion coefficients $\beta_2 = 0.53ps^2/km$ and $\beta_3 = 0.03ps^3/km$. The dashed black lines represent the simulation for the NLSE without TOD.

the experiments. Fig. 2a) shows the measured (shaded) and the calculated (lines) spectra for average input power of $P = 23dBm$ and $P = 25dBm$, showing a good agreement. The spectrum and the shape for an input pulse with $P = 23dBm$ propagating in a fiber without TOD is presented for comparison (dashed line). The spectrum at $P = 23dBm$ (experiment: dark shaded, simulation: red line) shows an asymmetry to the blue side, but also exhibits a broad pedestal on the red side. At $P = 25dBm$ (experiment: grey shaded, simulation: blue line) an increasing broadening of the pedestal is observed, which results in a broad Stokes peak at $1580nm$. The pulse shapes in Fig. 2b) show that pulse splitting at the leading edge sets in. The pulse-breakup phenomenon in the normal dispersion regime is described in [7]. The TOD leads to an asymmetric temporal development with an enhanced transfer of power from the trailing portion of the pulse to the leading one. The spectrum develops with a small asymmetric broadening towards the blue side. A narrow peak builds up and an increase of the peak intensity at the front of the pulse can be observed. Further propagation as well as a higher peak power leads to a sharp increase of the peak intensity at the front of the pulse, which is halted by temporal pulse splitting. After the splitting a small pedestal on the red side of the spectrum appears, which becomes more intensive with further propagation. The final spectrum of the pulse is asymmetric with a pronounced red tail. The HNLF used in the experiments exhibits a strong impact of TOD at the ZDW and has normal dispersion below $\lambda_0 = 1555$ nm, but has anomalous dispersion above this wavelength. The generated Stokes component is located in the anomalous dispersion regime, such that further propagation is now overlapped by soliton effects. To exclude the impact of possible anomalous dispersion on the observed phenomenon we changed to similar constellations of fiber coefficients with completely normal dispersion over the whole spectral range, which revealed qualitatively the same behavior. The critical

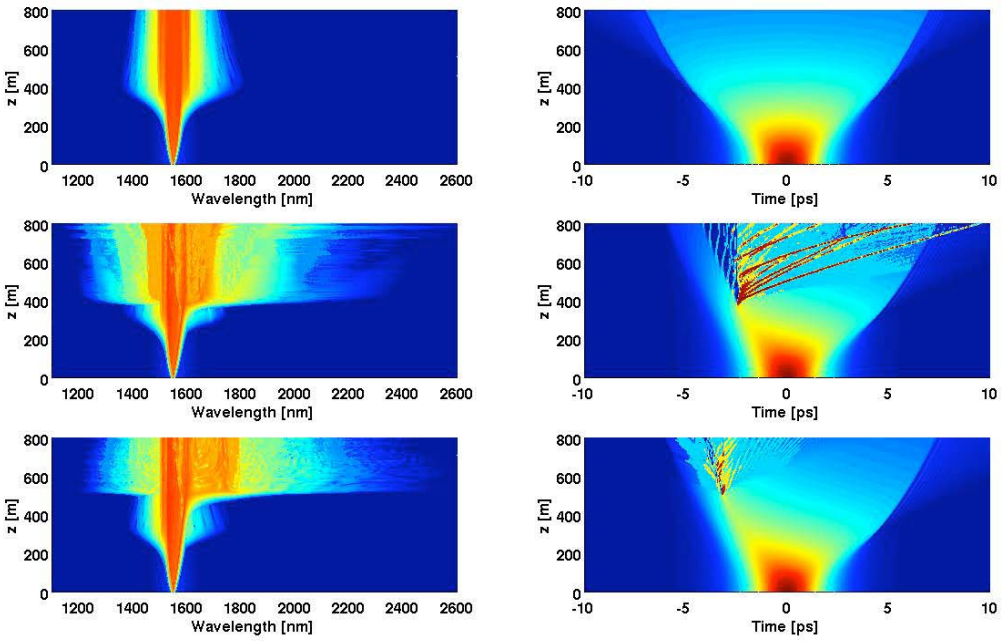

Figure 3: Spectral (left) and temporal (right) evolution of a pulse with initially $\tau_0 = 2.5ps$ and a peak power of $P_0 = 1.6W$ along $z = 800m$ HNLF with $\beta_2 = 0.2ps^2/km$ a,b) $\beta_3 = 0$, $\beta_4 = 0$, c,d) $\beta_3 = 0.01ps^3/km$, $\beta_4 = 0$, e,f) $\beta_3 = 0.01ps^3/km$, $\beta_4 = 1.7 \times 10^{-4}ps^4/km$.

distance z_{cr}, where the pulse splitting sets in, is proportional to the nonlinear length $L_{NL} = 1/(\gamma P_0)$ for fixed ratio L_D/L'_D with dispersion lengths $L_D = T_0^2/|\beta_2|$ and $L'_D = T_0^3/|\beta_3|$ [8]. Changing the dispersion coefficients now to $\beta_2 = 0.2ps^2/km$ and $\beta_3 = 0.01ps^3/km$ allows us to compare the behavior in the pure normal dispersion regime and the dynamics resulting from the intersection with the anomalos dispersion regime. The shift of the dispersion into the pure normal dispersion range can be achieved by switching on already a small value of β_4.

Fig. 3a,b) present the propagation for the pure NLSE without any impact of TOD. The pulse evolves first into a parabolic shape and broadens with further propagation nearly to a rectangular shape, thereby exhibiting optical wave breaking. The spectrum is then broadened by self-phase modulation. Introducing TOD for the same input pulse parameters leads to the pulse splitting phenomenon as described above. Fig. 3c,d) represent the case exhibiting normal and anomalous dispersion ($\beta_4 = 0$) and Fig. 3e,f) the case for normal dispersion over the whole spectral range ($\beta_4 = 1 \times 10^{-4}ps^4/km$). The propagation behavior coincides for both cases, until some of the broadened spectral components pass into the anomalous dispersion regime. In Fig. 3c,d) the FOD is set to zero, so that the Stokes component lies in the anomalous dispersion regime and soliton effects come into play. The further overall observed behavior is now mainly influenced by soliton fission and the generation of dispersive waves, leading to an additional blue shift in the spectrum [2, 3]. Soliton

effects are excluded in Fig. 3e,f), the spectral extension to the blue side through the transfer of energy to a resonant dispersive wave cannot be observed and the red-shift is more pronounced. The spectral width saturates after a certain propagation distance and remains in a well bounded domain with a fixed Stokes wavelength. With an increase of the input power the pulse splitting sets in at a shorter critical

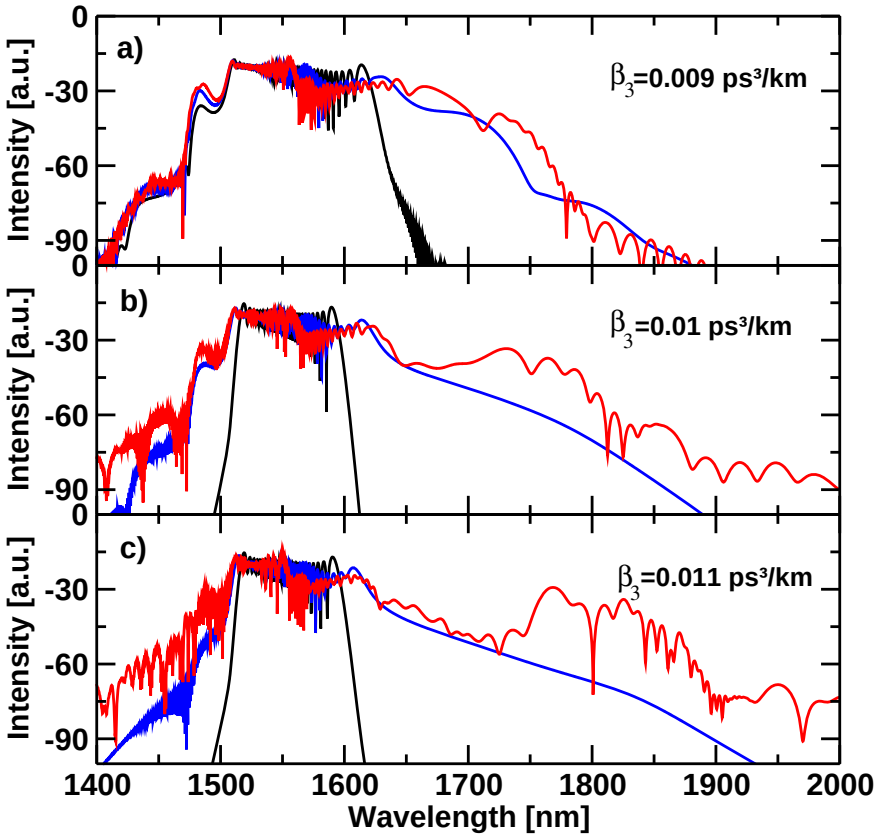

Figure 4: Spectra at $z = 170, 240, 280m$ for fixed input power $P_0 = 1.6W$ and pulse width $\tau_0 = 2.5ps$ at $\beta_2 = 0.2ps^2/km$ with increasing TOD.

distance z_{cr}, but does not lead to an enhanced spectral broadening to the red side. In comparison a further broadening to the red side can be observed by an slight increase of β_3. The wavelength of the Stokes component strongly depends on β_3. Fig. 4 shows the spectra with an increase of β_3. For $\beta_3 = 0.009ps^3/km$ (Fig. 4a) the Stokes component is located near the pump frequency and one observes only a small extension to the red side. With an increase of β_3 the Stokes component is shifted further into the red side (Fig. 4a,b)). Contrary to the Raman scattering, where the Stokes component is separated by $\sim 13THz$ from the pump frequency in fused silica, the Stokes component here can be adjusted to an arbitrary wavelength on the red side with an appropriate dispersion profile design.

In conclusion, we have demonstrated that the pulse breakup in the normal dispersion

regime induced by third-order dispersion generates new wavelengths on the red-side of the spectrum from the pump wavelength. This red-shift does not need explanations like the impact of higher-nonlinearities as Raman scattering or self-steepening, but follows from inherent properties of the NLSE with TOD as a perturbation. This represents a mechanism how even small values of higher-order dispersion can strongly affect the propagation dynamics in an optical fiber.

This work has been supported by DFG Research Center MATHEON.

References

[1] J. M. Dudley, G. Genty, and S. Coen, "Supercontinuum generation in photonic crystal fiber," Rev. Mod. Phys. **78**, 1135 – 1184 (2006).

[2] A.V. Husakou, and J. Herrmann, "Supercontinuum generation of higher-order-solitons by fission in photonic crystal fibers," Phys. Rev. Lett. **87**, 203901 (2001).

[3] A. Demircan, and U. Bandelow, "Analysis of the interplay between soliton fission and modulation instability in supercontinuum generation," Appl. Phys. B **86**, 31 – 39 (2007).

[4] G. P. Agrawal, *Nonlinear Fiber Optics* (Academic, San Diego, Calif.; 1995).

[5] S. Coen, A. H. L. Chau, R. Leonhardt, J. D. Harvey, J. C. Knight, W. J. Wadsworth, and P.St. J. Russel, "Supercontinuum generation by stimulated Raman scattering and parametric four-wave mixing in photonic crystal fibers," J. Opt. Soc. Am B. **19**, 753 – 764 (2002).

[6] U. Bandelow, A. Demircan and M. Kesting, "Simulation of pulse propagation in nonlinear optical fibers," WIAS Report **23** (2003).

[7] A. Demircan, M. Kroh, U. Bandelow, B. Hüttl, and H.-G. Weber, "Compresiion limit by third-order dispersion in the normal dispersion regime," IEEE Phot. Tech. Lett. **18**(22), 2353 –2355 (2006).

[8] A. Demircan, and U. Bandelow, "Limit for pulse compression by pulse splitting," Opt. Quant. Elect., in press.